This article has been accepted for publication in a future issue of this journal, but has not been fully edited. Content may change prior to final publication.
Citation information: DOI: 10.1109/lsp.2025.3612359,

Delay Coprime Array: A New Sparse Linear Array for Fast and Robust DOA Estimation

Jiahui Cao, *Graduate Student Member, IEEE*, Zhibo Yang, *Member, IEEE*, Ming Xiao, *Senior Member, IEEE*, Xuefeng Chen, *Senior Member, IEEE*, Asoke K. Nandi, *Life Fellow, IEEE*,

***Abstract*—In this letter, we propose a new sparse linear array (SLA), termed delay coprime array (DCA), and correspondingly develop a low-complexity direction of arrival (DOA) estimation algorithm. In terms of structure, unlike existing SLAs, e.g., coprime array, DCA is composed of two "large-spaced" uniform linear arrays (ULAs) with shifted distance which is coprime with the inter-element spacing in the ULAs. In terms of algorithm, the proposed algorithm involves ambiguity and de-ambiguity stages and significantly improves estimation accuracy due to the active use of phase ambiguity instead of hastily suppressing ambiguity. Numerical results indicate that DOA estimation with DCA has comparable performance as the existing DOA estimation with SLAs, but with much lower complexity and simpler configuration. Admittedly, since the proposed method achieves fast calculation without using difference co-array, it losts the ability to identify more sources. Yet, owing to low complexity and simple configuration, DCA and the corresponding algorithm are expected to play a role in DOA estimation.**

***Index Terms*—Sparse linear array, DOA estimation, phase ambiguity, phase de-ambiguity, Chinese remainder theorem.**

I. Introduction

DIRECTION of arrival (DOA) estimation is a fundamental problem in array signal processing and has diverse applications in radar, sonar, radio astronomy, and wireless communications [1]–[6]. Based on the generic restriction given in the Shannon-Nyquist sampling theorem [7], uniform linear array (ULA) has become the most prevalent array geometry where the inter-element spacing is set to be half-wavelength such that the DOA can be estimated without ambiguity. However, due to the small spacing, ULA suffers from severe mutual coupling between sensors and is expensive to achieve a large array aperture for fine estimation resolution [8], [9]. To overcome these limitations, recently various sparse linear arrays (SLAs) have proposed, e.g., minimum redundancy array, coprime array (CA), nested array (NA), and their variants [10]–[16]. Minimum redundancy array requires complex configuration. Although CA and NA are easy to design, they may still suffer from severe mutual coupling effect due to the presence of dense local arrays. To solve this problem, super nested array (SNA) [17] has been proposed by rearranging the dense uniform subarrays in NA. Moreover, thinned coprime array (TCA) [18] has been developed by exploiting the redundancy in difference co-array domain of CA. Inspired by both NA and CA, coprime nested array (CNA) [19] has been proposed using the nesting property of CA. However, almost all DOA estimation with SLAs are conducted in the difference co-array domain and involve massive computations. To reduce computation, some low-complexity algorithms have been developed based on CA [20], [21], which perform ESPRIT on the sparse ULAs in CA separately and estimate the true DOA from the ambiguous phases by observing all possible estimations from two sparse ULAs. However, those algorithms are only applicable to CA and cannot obtain closed-form solutions.

Inspired by our previous work on undersampling frequency estimation [22], [23], we propose a novel and simple sparse array, termed delay coprime array (DCA) and correspondingly develop a low-complexity DOA estimation algorithm. In terms of structure, DCA is the superposition of two sparse ULAs with a shifted distance which is coprime with the inter-element spacing in the ULAs. In terms of algorithm, the proposed estimation algorithm consists of Unitary-ESPRIT-based phase ambiguity stage and Chinese remainder theorem (CRT)-based phase de-ambiguity stage, and it significantly improves estimation accuracy due to the active use of phase ambiguity. Numerical results have shown that DOA estimation with DCA has comparable performance to the existing SLAs, yet with much lower complexity and simpler configuration.

Notations: we use $\gcd(\cdot)$ and $\mathrm{lcm}(\cdot)$ to represent greatest common divisor and least common multiple, respectively. The phase superscript "a" (ϕ^a) denotes the ambiguous version of the true phase ϕ, and the difference between them is an integer multiple of 2π. The unit distance d of arrays is set to be half-wavelength. A variable with hat denotes an estimate with error.

II. Preliminaries

The schematic diagram of classic far-field DOA estimation is shown in Fig. 1, where the two circles represent array sensors with distance d, and the solid line is the signal source with DOA θ. Without loss of generality, assume the signal source is as follows

$$s(t) = A\exp(j2\pi f_0 t + j\varphi) + w(t), \tag{1}$$

where A, f_0, and φ respectively denote the amplitude, frequency, and phase of the signal. $w(t)$ is measurement noise.

From Fig. 1, there is a delay τ between the signal's time of arrival to the two sensors. Then, the delay τ results in a phase difference ϕ between the received signals by the two sensors,

$$\tau = d\sin\theta/c, \quad \phi = 2\pi f_0 \tau, \tag{2}$$

This work was supported by the National Natural Science Foundation of China (Nos. 523B2044, 92360306, and 52241502). The work of Nandi Asoke was supported in part by the Royal Society award (No. IEC\NSFC\223294) (Corresponding author: Z. Yang). J. Cao, Z. Yang, and X. Chen are with the National Key Lab of Aerospace Power System and Plasma Technology, Xi'an Jiaotong University, Xi'an 710049, China (e-mail: caojiahui@stu.xjtu.edu.cn; phdapple@mail.xjtu.edu.cn). M. Xiao is with the Department of Communication Theory, Royal Institute of Technology, 100 44 Stockholm, Sweden (e-mail: mingx@kth.se). Asoke K. Nandi is with the Department of Electronic and Electrical Engineering, Brunel University of London, UB8 3PH Uxbridge, U.K. (e-mail: Asoke.Nandi@brunel.ac.uk).

This article has been accepted for publication in a future issue of this journal, but has not been fully edited. Content may change prior to final publication.
Citation information: DOI: 10.1109/lsp.2025.3612359,

where c denotes the speed of electromagnetic waves. Let λ

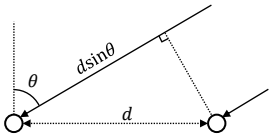

Fig. 1. Schematic diagram of DOA estimation.

denotes the signal wavelength. Substituting $f_0 = c/\lambda$ into (2), the phase difference ϕ can be rewritten as

$$\phi = 2\pi d \sin\theta/\lambda. \tag{3}$$

Eq. (3) is a fundamental formula of DOA estimation. By (3), DOA estimation is equivalent to phase difference estimation since $\theta = \arcsin\left(\frac{\phi\lambda}{2\pi d}\right)$. In practice, the calculated phase difference is limited to $(-\pi, \pi]$. In order to ensure the equivalence between the calculated and true phase differences, the distance d is required to satisfy $d \leqslant \lambda/2$. Furthermore, reducing d will widen the main-lobe and thus lead to poor directionality/resolution. Thus, d is generally set to be half-wavelength ($d = \lambda/2$) in the field of DOA. In the following Sections III and IV, we respectively introduce the proposed DCA and corresponding DOA estimation algorithm.

III. Delay Coprime Array

The proposed DCA is the superposition of two unconventional ULAs with a large distance, as depicted in Fig. 2. Note that, the distance of inner sensors in the two ULAs is $(P+Q)d$ and there exists a shifted distance Pd between the two ULAs. Particularly, $\gcd(P, Q) = 1$ in DCA. Without loss of generality, let $P < Q$. It should be emphasized that although the name of DCA is similar to CA, DCA is completely different from CA in terms of both array structure and estimation algorithm. DCA is the new paradigm of our previous work "delay coprime sampling" [22], [24] in the spatial domain. Strictly, DCA is the superposition of two large-spaced ULAs with a shifted distance where the shifted distance and the uniform spacing are coprime. By definition, it may be more appropriate to refer to this array as "spacing coprime array". However, herein this array as shown in Fig. 2 is still referred to as "delay coprime array" for consistency.

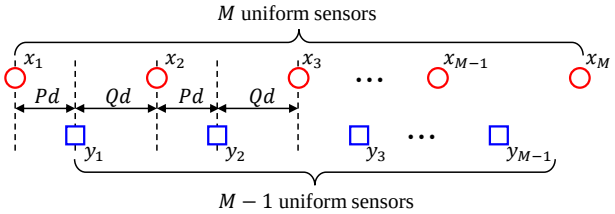

Fig. 2. Delay coprime array. Note that P and Q are coprime numbers.

For ease of expression, assume there are $2M-1$ sensors in DCA, that is, the two uniform subarrays in DCA respectively contain M and $M-1$ sensors (see Fig. 2). Let $\{x_1(n), x_2(n), \cdots, x_M(n)\}_{n=1}^N$ and $\{y_1(n), y_2(n), \cdots, y_{M-1}(n)\}_{n=1}^N$ denote the measured discrete data by the first and second uniform subarrays, respectively, and N denotes the number of snapshots. In addition, $M-1$ is required to be smaller than the number of sources.

IV. Two Stages DOA Estimation with DCA

In this section, we present the DOA estimation with DCA in two stages: ambiguity and de-ambiguity stages.

A. Ambiguity Stage: Mining Ambiguous Phases

Phase difference (hereinafter abbreviated as phase), is closely related to delay [see (2)]. In the first stage, we construct different delay schemes to calculate phases.

Firstly, we construct the first delay scheme by forming snapshots as follows

$$\text{Scheme 1:} \begin{cases} \boldsymbol{x_1}(n) = [x_1(n), x_2(n), \cdots, x_{M-1}(n)]^{\mathrm{T}} \\ \boldsymbol{y_1}(n) = [y_1(n), y_2(n), \cdots, y_{M-1}(n)]^{\mathrm{T}} \end{cases}, \tag{4}$$

where $\boldsymbol{x_1}(n)$ and $\boldsymbol{y_1}(n)$ denote the snapshots from the subarray 1 and subarray 2 in the first delay scheme, as shown in Fig. 3. Readily, the delay and phase (difference) between the two snapshots in the first scheme respectively are

$$\tau_1 = P\frac{\lambda}{2}\sin\theta/c, \quad \phi_1 = P\pi\sin\theta. \tag{5}$$

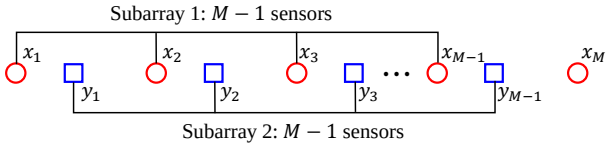

Fig. 3. The first delay scheme.

Then, the second delay scheme is constructed as follows

$$\text{Scheme 2:} \begin{cases} \boldsymbol{x_2}(n) = [y_1(n), y_2(n), \cdots, y_{M-1}(n)]^{\mathrm{T}} \\ \boldsymbol{y_2}(n) = [x_2(n), x_3(n), \cdots, x_M(n)]^{\mathrm{T}} \end{cases}, \tag{6}$$

where $\boldsymbol{x_2}(n)$ and $\boldsymbol{y_2}(n)$ denote the snapshots from the subarray 1 and subarray 2 in the second delay scheme, as shown in Fig. 4. Readily, the delay and phase (difference) between the two snapshots in the second scheme respectively are

$$\tau_2 = Q\frac{\lambda}{2}\sin\theta/c, \quad \phi_2 = Q\pi\sin\theta. \tag{7}$$

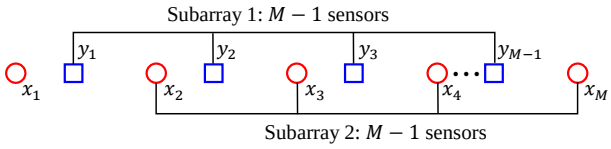

Fig. 4. The second delay scheme.

The above-mentioned phases (ϕ_1, ϕ_2) are the true phases which may be out of the computable range $(-\pi, \pi]$ because $Q > P \geqslant 1$. That is, the calculated phases are the ambiguous versions of the true phases,

$$\phi_1 = 2\pi n_1 + \phi_1^a, \quad \phi_2 = 2\pi n_2 + \phi_2^a, \tag{8}$$

where ϕ_1^a and ϕ_2^a denotes the ambiguous phases of ϕ_1 and ϕ_2, respectively, which can be calculated by existing methods, e.g., ESPRIT and its variants [23]. n_1 and n_2 are unknown integers called ambiguity integers.

This article has been accepted for publication in a future issue of this journal, but has not been fully edited. Content may change prior to final publication.
Citation information: DOI: 10.1109/lsp.2025.3612359,

B. De-ambiguity Stage: Reconstructing True Phase

To estimate DOA accurately, we then determine the true phases according to the ambiguous phases in the second stage.

By substituting $\phi_1 = P\pi \sin\theta$ and $\phi_2 = Q\pi \sin\theta$ into (8), we have the following simultaneous equations

$$\begin{cases} P\pi \sin\theta = 2\pi n_1 + \phi_1^a \\ Q\pi \sin\theta = 2\pi n_2 + \phi_2^a \end{cases}. \tag{9}$$

Then (9) can be rewritten as follows

$$\text{Congruence equation: } \begin{cases} \frac{PQ}{2}\sin\theta = Qn_1 + \frac{Q\phi_1^a}{2\pi} \\ \frac{PQ}{2}\sin\theta = Pn_2 + \frac{P\phi_2^a}{2\pi} \end{cases}. \tag{10}$$

When $\frac{PQ}{2}\sin\theta$ may be a negative value which contradicts the non-negative dividend requirement in the traditional congruence equation, we define a new number $X \triangleq \frac{PQ}{2}(1+\sin\theta)$. Then, (10) can be equivalently written as

$$\begin{cases} X = Qn_1 + \frac{Q\phi_1^a}{2\pi} + \frac{PQ}{2} \\ X = Pn_2 + \frac{P\phi_2^a}{2\pi} + \frac{PQ}{2} \end{cases}, \tag{11}$$

where $\{P, Q\}$ and $\{\frac{Q\phi_1^a}{2\pi} + \frac{PQ}{2}, \frac{P\phi_2^a}{2\pi} + \frac{PQ}{2}\}$ respectively are the moduli and remainders. X is here dividend, particularly, here it is the number to reconstruct. According to CRT [25], [26], X can be uniquely reconstructed since

$$X \triangleq \frac{PQ}{2}(1+\sin\theta) \leqslant PQ = \mathrm{lcm}\{P, Q\}, \tag{12}$$

where the last equality come from the fact $\gcd(P, Q) = 1$. This explains the reason why we require $\gcd(P, Q) = 1$.

Furthermore, note that, although the remainders in (11) are not strict remainder in mathematical sense since they are non-integers and greater than moduli, X can be reconstructed by variant CRT algorithms, e.g., robust CRT (RCRT) [27]–[29]. Then, by the definition of X, the DOA estimation is achieved by

$$\hat{\theta} = \arcsin(2\hat{X}/(PQ) - 1), \tag{13}$$

where $\hat{X}$ denotes the reconstruction/estimation of X, and $\hat{\theta}$ denotes the estimation of θ.

Remarkably, while the above derivation is based on a single source, extension to multiple-source cases is straightforward since the ambiguous phases and the multiple sources have one-to-one correspondences in Unitary-ESPRIT [21]. Thereby, the multiple-DOA estimation can be simplified to multiple single-DOA estimations once the ambiguous phases are calculated.

As a summary, the complete flow is given in Algorithm 1.

Algorithm 1: Two stages DOA Estimation with DCA

Input: Received data: $\{x_m(n)\}_{n=1}^N$ and $\{y_m(n)\}_{n=1}^N$ for $m = 1, 2, \cdots, M$; Number of sources: K;
Output: DOA estimations: $\{\hat{\theta}_k\}_{k=1}^K$

1 Construct two delay schemes according to (4) and (6);
2 Calculate ambiguous phases $\{\hat{\phi}_1^a(k), \hat{\phi}_2^a(k)\}_{k=1}^K$ corresponding to K sources by Unitary-ESPRIT;
3 Build congruences (11) and reconstruct X via RCRT;
4 Estimate DOA by (13): $\hat{\theta}_k = \arcsin(2\hat{X}/(PQ) - 1)$.

V. Error Analysis

In this section, we will demonstrate the advantage of the proposed DCA in estimation accuracy by comparing it with a ULA with the same number of sensors.

In ULA, DOA is directly estimated by

$$\text{ULA: } \hat{\theta}_{\text{ULA}} = \arcsin(\hat{\phi}/\pi), \tag{14}$$

where $\hat{\phi}$ denotes the estimated phase by a certain method, e.g., ESPRIT. Note that $\hat{\phi}$ is free from phase ambiguity.

Let Δe be the average error of the aforementioned phase estimations $(\hat{\phi}, \hat{\phi}_1^a, \hat{\phi}_2^a)$. Then, the error of variable $\hat{\phi}/\pi$ is

$$\delta(\sin(\hat{\theta}_{\text{ULA}})) = \delta\left(\hat{\phi}/\pi\right) = \frac{\Delta e}{\pi}, \tag{15}$$

where $\delta(\cdot)$ denotes the error of a certain variable.

In DCA, DOA estimation is achieved by

$$\begin{aligned} &\text{DCA: } \hat{\theta}_{\text{DCA}} = \arcsin(2\hat{X}/(PQ) - 1) \\ &= \arcsin\left(\frac{P\hat{n}_2 + Q\hat{n}_1}{PQ} + \frac{\hat{\phi}_1^a}{2\pi P} + \frac{\hat{\phi}_2^a}{2\pi Q} - 1\right), \end{aligned} \tag{16}$$

where $\hat{n}_1$ and $\hat{n}_2$ denotes estimations of n_1 and n_2. In particular, it has been proven that $\hat{n}_1$ and $\hat{n}_2$ obtained by RCRT are precisely n_1 and n_2 when the remainder errors are less than 1/4 [27]. Based on this prerequisite, the estimation error of $\hat{\theta}_{\text{DCA}}$ is caused by ambiguous phase estimations $\hat{\phi}_1^a$ and $\hat{\phi}_2^a$. From (16), the estimation error of $\sin(\hat{\theta}_{\text{DCA}})$ is

$$\delta(\sin(\hat{\theta}_{\text{DCA}})) = \delta\left(\frac{Q\hat{\phi}_1^a + P\hat{\phi}_2^a}{2\pi PQ}\right) = \frac{\Delta e}{\pi}\cdot\frac{\sqrt{P^2+Q^2}}{2PQ}, \tag{17}$$

where the last equality comes from the error propagation formulation under the i.i.d. assumption. Note that $\delta(\hat{\phi}_1^a)$ and $\delta(\hat{\phi}_2^a)$ are assumed to be Δe.

Since $Q > P \geqslant 1$, it is easily verified that

$$\delta(\sin(\hat{\theta}_{\text{DCA}})) < \delta(\sin(\hat{\theta}_{\text{ULA}})). \tag{18}$$

Eq. (18) indicates that the estimation error of DCA is less than that of ULA. In particular, according to (17), the estimation error of DCA will significantly decrease as P and Q increase if the ambiguity integers (n_1, n_2) are precisely determined. However, does this imply we should fanatically choose large P and Q in DCA? The answer is clearly negative. To explain the reason, we need to review the condition that we take for granted: n_1 and n_2 can be precisely determined via RCRT if and only if the remainder errors are less than 1/4 [27], i.e., the condition for a robust reconstruction

$$\max\left\{\delta\left(\frac{Q\hat{\phi}_1^a}{2\pi}\right), \delta\left(\frac{P\hat{\phi}_2^a}{2\pi}\right)\right\} < \frac{1}{4}. \tag{19}$$

Substituting $\delta(\hat{\phi}_1^a), \delta(\hat{\phi}_2^a) = \Delta e$ into (19), we have

$$\Delta e < \frac{\pi}{2\max\{P, Q\}} = \frac{\pi}{2Q}. \tag{20}$$

Therefore, in practice, choosing larger P and Q will result in higher risks that ambiguity integers are incorrectly determined and then lead to unacceptable DOA estimation errors. Thus, the selection of P and Q should consider both the propagation error (17) and the condition for a robust reconstruction (19).

This article has been accepted for publication in a future issue of this journal, but has not been fully edited. Content may change prior to final publication.
Citation information: DOI: 10.1109/lsp.2025.3612359,

VI. Numerical Simulations

In this section, we conduct numerical simulations to verify the effectiveness of DCA by comparing with ULA and classic SLAs including SNA [17], TCA [18], and CNA [19]. The number of sensors in all arrays is set to 19. The configurations for DCA are $P = 7$ and $Q = 9$ and the configurations for other SLAs are set to be respectively optimal. In addition, Algorithm 1 and ESPRIT are used in DOA estimation with DCA and ULA, respectively. Other SLAs extract the largest portion of consecutive lags from the available segments of consecutive lags in the co-array followed by the spatial smoothing technique to generate the covariance matrix based on the extracted co-array segment before applying ESPRIT. In the simulations, the noise is added to be zero-mean additive white Gaussian process, and a total of 200 random tests are conducted. The number of snapshots is set to be $N = 100$.

For the ease of comparison, Fig. 5(a) plots the RMSE performance of different arrays versus SNR, where there are two uncorrelated sources with unit amplitudes ($A = 1$) and different DOAs $(20°, 65°)$. Readily, in low SNRs ($\leqslant -5$ dB), the performance of DCA is admittedly unsatisfactory. This is mainly caused by the failed reconstruction due to unacceptable ambiguous phase errors. In the DOA estimation with DCA, an RCRT-based de-ambiguity algorithm is used to reconstruct the true phase from ambiguous phases and it will fail when the remainder error exceeds 1/4. However, when SNR is higher than 0 dB, DCA is significantly superior to the ULA. This is mainly owing to the two-stage estimation strategy and the reduced correlation of the subarrays. Moreover, DCA performs better than the other SLAs, especially in high SNRs. Therefore, according to our experiences, it is recommended to use DCA when SNR is higher than 0 dB. Remarkably, it should be emphasized that the main advantage of DCA over other SLAs is its low computational complexity for DOA estimation.

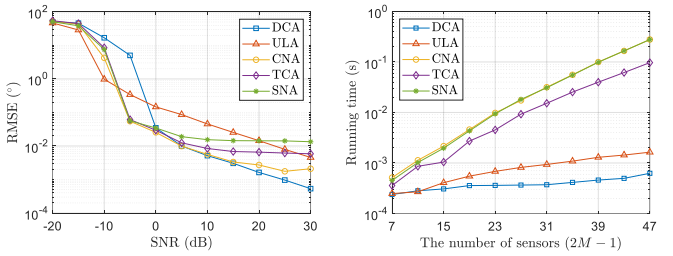

(a) (b)

Fig. 5. Comparison of different arrays: (a) RMSEs versus SNR; (b) running time versus the number of sensors.

Fig. 5(b) shows the complexity comparison of all arrays under different array sizes. All results are obtained using an ordinary computer with 2.9 GHz CPU i5-10400F, 32 GB RAM, and MATLAB 2019a. The number of sensors $(2M-1)$ varies from 7 to 47. Other simulation parameters are consistent with the previous simulation. It is readily seen that the computational complexity of DOA estimation algorithm with DCA is the least, it is a bit lower than that with ULA and much lower than those with SLAs. Although the proposed DOA estimation algorithm with DCA involves two ESPRIT-based calculations for ambiguous phases, its running time is still slightly faster than the ESPRIT-based calculation with ULA because its subarrays for ESPRIT have smaller sizes. Furthermore, since the DOA estimation algorithm with conventional SLAs requires excessive difference operations and spatial smoothing, their running time is much longer than the proposed method with DCA. However, it should be noted that in addition to a sparse configuration, another major advantage of existing SLAs is their ability to identify more sources, which is lacking in the proposed method with DCA since it doesn't operate on the difference co-array domain.

From Fig. 5, we have seen the performance of DCA with $P = 7$ and $Q = 9$. It has been revealed in Section V that DCA's robustness to noise is closely related to the selection of P and Q. To study the impact of P and Q on the performance of DCA, we plot RMSEs of DCAs with different configurations versus SNR in Fig. 6(a). It is readily seen that the RMSEs of DCA decrease in high SNRs ($\geqslant 0$ dB) but increase in low SNRs ($\leqslant -5$ dB) as the P and Q increase. As said at the end of Section V, the optimal selection of P and Q should balance between estimation accuracy and robustness. Specifically, in high SNRs, the DCA with larger P and Q are recommended for pursuing high estimation accuracy; while in low SNRs, the DCA with smaller P and Q should be considered to ensure a robust reconstruction [30]. In addition, Fig. 6(b) plots the RMSEs of different DCAs versus the number of snapshots (N) in the case of SNR = 5 dB. Admittedly, the estimation accuracies of DCAs gradually increase with the increase of N; however, they are very limited, especially for $N \geqslant 300$. In other words, DCA can achieve high-accuracy estimation without a larger number of snapshots.

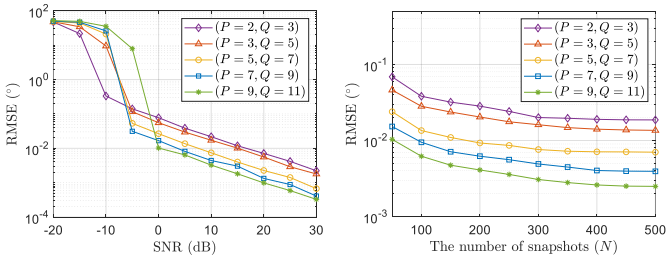

(a) (b)

Fig. 6. RMSEs of DCAs with different P and Q versus (a) SNR and (b) N.

VII. Concluding Remarks

In this letter, we have proposed a new SLA, termed DCA, and correspondingly develop a two-stage DOA estimation. In terms of structure, DCA is the superposition of two large-spaced ULAs with a shifted distance where the shifted distance and the uniform spacing are coprime. In terms of algorithm, the proposed estimation algorithm involves ambiguity and de-ambiguity stages and significantly improves estimation accuracy due to the active use of phase ambiguity. Numerical results have shown that DOA estimation with DCA has comparable performance as the existing DOA estimation with SLAs, but with much lower complexity and simpler configuration.

This letter can be regarded as a basic introduction to DCA. Currently, DCA is only applicable to uncorrelated sources and narrowband signal. Its applicability could be extended by incorporating existing techniques, e.g., spatial smoothing. Moreover, further performance analysis considering mutual coupling is worthwhile in the future.

This article has been accepted for publication in a future issue of this journal, but has not been fully edited. Content may change prior to final publication. Citation information: DOI: 10.1109/lsp.2025.3612359,

REFERENCES

[1] H. Krim and M. Viberg, "Two decades of array signal processing research: the parametric approach," *IEEE Signal Process. Mag.*, vol. 13, no. 4, pp. 67–94, 1996.

[2] X. Zhang, L. Xu, L. Xu, and D. Xu, "Direction of departure (dod) and direction of arrival (doa) estimation in mimo radar with reduced-dimension music," *IEEE Commun. Lett.*, vol. 14, no. 12, pp. 1161–1163, 2010.

[3] S. Qin, Y. D. Zhang, and M. G. Amin, "Generalized coprime array configurations for direction-of-arrival estimation," *IEEE Trans. Signal Process.*, vol. 63, no. 6, pp. 1377–1390, 2015.

[4] M. Xiao, S. Mumtaz, Y. Huang, L. Dai, Y. Li, M. Matthaiou, G. K. Karagiannidis, E. Björnson, K. Yang, I. Chih-Lin *et al.*, "Millimeter wave communications for future mobile networks," *IEEE J. Sel. Area. Commun.*, vol. 35, no. 9, pp. 1909–1935, 2017.

[5] Y. Yuan, S. Wu, M. Wu, and N. Yuan, "Unsupervised learning strategy for direction-of-arrival estimation network," *IEEE Signal Process. Lett.*, vol. 28, pp. 1450–1454, 2021.

[6] Z. Xu, Y. Chen, and P. Zhang, "A sparse uniform linear array doa estimation algorithm for fmcw radar," *IEEE Signal Process. Lett.*, vol. 30, pp. 823–827, 2023.

[7] A. Pizzo, A. de Jesus Torres, L. Sanguinetti, and T. L. Marzetta, "Nyquist sampling and degrees of freedom of electromagnetic fields," *IEEE Trans. Signal Process.*, vol. 70, pp. 3935–3947, 2022.

[8] C. Zhou and J. Zhou, "Direction-of-arrival estimation with coarray esprit for coprime array," *Sensors*, vol. 17, no. 8, p. 1779, 2017.

[9] Z. Ye, J. Dai, X. Xu, and X. Wu, "Doa estimation for uniform linear array with mutual coupling," *IEEE Trans. Aerosp. Electron. Syst.*, vol. 45, no. 1, pp. 280–288, 2009.

[10] A. Moffet, "Minimum-redundancy linear arrays," *IEEE Trans. Antenn. Propag.*, vol. 16, no. 2, pp. 172–175, 1968.

[11] P. Pal and P. P. Vaidyanathan, "Nested arrays: A novel approach to array processing with enhanced degrees of freedom," *IEEE Trans. Signal Process.*, vol. 58, no. 8, pp. 4167–4181, 2010.

[12] P. P. Vaidyanathan and P. Pal, "Sparse sensing with co-prime samplers and arrays," *IEEE Trans. Signal Process.*, vol. 59, no. 2, pp. 573–586, 2010.

[13] J. Liu, Y. Zhang, Y. Lu, S. Ren, and S. Cao, "Augmented nested arrays with enhanced dof and reduced mutual coupling," *IEEE Trans. Signal Process.*, vol. 65, no. 21, pp. 5549–5563, 2017.

[14] Z. Zheng, W.-Q. Wang, Y. Kong, and Y. D. Zhang, "Misc array: A new sparse array design achieving increased degrees of freedom and reduced mutual coupling effect," *IEEE Trans. Signal Process.*, vol. 67, no. 7, pp. 1728–1741, 2019.

[15] S. Ren, W. Dong, X. Li, W. Wang, and X. Li, "Extended nested arrays for consecutive virtual aperture enhancement," *IEEE Signal Process. Lett.*, vol. 27, pp. 575–579, 2020.

[16] J. Cao, Z.-b. Yang, G. Teng, and X. Chen, "Coprime and nested samplings-based spectrum reconstruction in blade tip timing," *Mechanical Systems and Signal Processing*, vol. 186, p. 109887, 2023.

[17] C.-L. Liu and P. Vaidyanathan, "Super nested arrays: Linear sparse arrays with reduced mutual coupling—part i: Fundamentals," *IEEE Trans. Signal Process.*, vol. 64, no. 15, pp. 3997–4012, 2016.

[18] A. Raza, W. Liu, and Q. Shen, "Thinned coprime array for second-order difference co-array generation with reduced mutual coupling," *IEEE Trans. Signal Process.*, vol. 67, no. 8, pp. 2052–2065, 2019.

[19] Z. Peng, Y. Ding, S. Ren, H. Wu, and W. Wang, "Coprime nested arrays for doa estimation: Exploiting the nesting property of coprime array," *IEEE Signal Process. Lett.*, vol. 29, pp. 444–448, 2021.

[20] F. Sun, B. Gao, L. Chen, and P. Lan, "A low-complexity esprit-based doa estimation method for co-prime linear arrays," *Sensors*, vol. 16, no. 9, p. 1367, 2016.

[21] J. Li, D. Jiang, and X. Zhang, "Doa estimation based on combined unitary esprit for coprime mimo radar," *IEEE Commun. Lett.*, vol. 21, no. 1, pp. 96–99, 2016.

[22] J. Cao, Z. Yang, and X. Chen, "Delay coprime sampling: A simplified sub-nyquist sampling for noisy multi-sinusoidal signals," *IEEE Signal Process. Lett.*, vol. 31, pp. 1720–1724, 2024.

[23] J. Cao, Z. Yang, M. Lu, L. Lu, and X. Chen, "Active aliasing esprit: A robust parameter estimation method for low-intervention blade tip timing measurement," *IEEE Trans. Signal Process.*, vol. 227, p. 112392, 2025.

[24] J. Cao, Z. Yang, R. Sun, and X. Chen, "Delay sampling theorem: A criterion for the recovery of multitone signal," *Mech. Syst. Signal Process.*, vol. 200, p. 110523, 2023.

[25] X.-G. Xia and G. Wang, "Phase unwrapping and a robust chinese remainder theorem," *IEEE Signal Process. Lett.*, vol. 14, no. 4, pp. 247–250, 2007.

[26] J. Cao, Z. Yang, S. Tian, H. Li, R. Jin, R. Yan, and X. Chen, "Biprobes blade tip timing method for frequency identification based on active aliasing time-delay estimation and dealiasing," *IEEE Trans. Ind. Electron.*, vol. 70, no. 2, pp. 1939–1948, 2022.

[27] W. Wang and X.-G. Xia, "A closed-form robust chinese remainder theorem and its performance analysis," *IEEE Trans. Signal Process.*, vol. 58, no. 11, pp. 5655–5666, 2010.

[28] J. Cao, Z. Yang, S. Tian, G. Teng, and X. Chen, "Active aliasing technique and risk versus error mechanism in blade tip timing," *Mech. Syst. Signal Process.*, vol. 191, p. 110150, 2023.

[29] J. Cao, Z. Yang, R. Sun, and X. Chen, "From theory to practice: Chinese remainder theorem-based blade tip timing measurement," *IEEE Transactions on Instrumentation and Measurement*, vol. 74, p. 3520910, 2025.

[30] J. Cao, Z. Yang, and A. K Nandi, "Grouping and sifting chinese remainder theorem for frequency estimation of undersampled waveforms avoiding multi-rate sampling," vol. Available at SSRN: https://ssrn.com/abstract=5221177.